

# Width and shift of the He II Balmer- $\alpha$ line in a dense z-pinch plasma

R. Ahmad<sup>a</sup>

Centre for Advanced Studies in Physics, Government College Lahore, Pakistan

Received: 30 October 1998 / Received in final form: 20 March 1999

**Abstract.** The measurement of the width and shift of the He II Balmer- $\alpha$  line is reported in this paper. The monochromator used in the detection system was calibrated in wavelength by using a low-density hollow-cathode lamp emitting the He II Balmer- $\alpha$  line. The effect of the radial gradients on the shift and width is also corrected.

**PACS.** 52.90.+z Other topics in physics of plasmas and electric discharges

## 1 Introduction

The importance of the Stark broadened line profile is well established [1,2]. Lines of ionised helium are of great importance and exist in O-type stars and central stars of nebulae [3]. To date many attempts have been carried out to calculate and measure the lines of the singly ionised helium. Spectral lines from ions have long been known to be shifted by the interactions with charged particles in a plasma. However, the agreement of shift calculations with measurements is usually less satisfactory than in the case of line widths. The magnitude of the shifts of hydrogenic ion lines in a dense plasma remains a controversial subject both theoretically and experimentally [4–9]. Therefore it still remains an interesting and challenging problem because of its  $n$ -body nature. The exact wavelengths of spectral lines of highly charged ions are required in the determination of line opacities and level positions for X-ray laser transitions which is ultimately used in the calculations of the gain. The shifts are also important from an astrophysical point of view in connection with the relativistic gravitational red shift [10].

Previously, workers [7,11–13] have measured the line profile of the He II Balmer-alpha. All these measurements were made at densities around  $10^{17}$  cm<sup>-3</sup> except Marangos *et al.* [12] and Ahmad [14] which are an order of magnitude less than our work. Marangos *et al.* measured the line for only one plasma condition without any analysis. The work presented in this paper bears new analysis in the case of width of the line from earlier work [14] and a study of shift of the line presented here has never been published before.

## 2 Experimental description

The experimental arrangement is shown in Figure 1. The plasma was produced in a z-pinch and high peak densities were partly available due to the construction of the capacitor bank from low-induction feeding lines. The dimension of the discharge tube is 100 m in diameter and 200 m long and is made of Pyrex glass. The detail of the z-pinch can be found in references [12,15]. The line shapes are observed along the line of sight and averaged over ten shots at each wavelength position. The plasma is inhomogeneous because of its small size. At the peak compression, the plasma column is fairly homogeneous. Therefore lines were observed at the time of peak compression (6  $\mu$ s in our case) when the plasma was confined to a narrow cylinder few millimetre in diameter. High-purity helium gas (less than 1 ppm hydrogen) was used in the z-pinch. Helium gas was continuously flowing through the system during the experimental run. This continuous flow of the gas helps to reduce the impurity level in the source. The shot-to-shot reproducibility of the z-pinch was found to be 7%.

The electron density was measured using spatially resolved Mach-Zehnder interferometry with argon-ion laser perpendicular to the axis of the plasma [16,17]. Spatially resolved electron densities were obtained using Abel Inversion and peak plasma density varied between 1.3 and  $3.5 \times 10^{18}$  cm<sup>-3</sup> with spatial half-half-width of 0.75 mm and error of  $\pm 20\%$ . Spatially resolved temperature diagnostic was not possible due to the narrow width of the plasma column. The temperature was deduced using the intensity ratio of the He II 5876 Å and He II 4686 Å spectral line intensities. The line-of-sight averaged temperatures were found to be between 2.7 and  $3.8 \pm 0.2$  K increasing with increasing density. It certainly has large systematic uncertainties (Tab. 1).

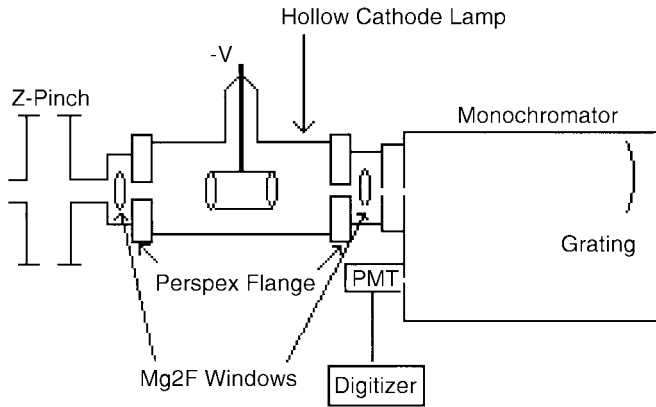
All earlier line position measurements [11] were made with reference to impurity lines but we used in preference

---

<sup>a</sup> e-mail: ahriaz@hotmail.com

**Table 1.** The values of peak electron densities and temperature.

$N_e (\times 10^{18} \text{ cm}^{-3})$	1.32	1.76	1.85	2.15	2.9	3.5
$T_e$ (K)	29500	32200	27200	33200	33600	38400

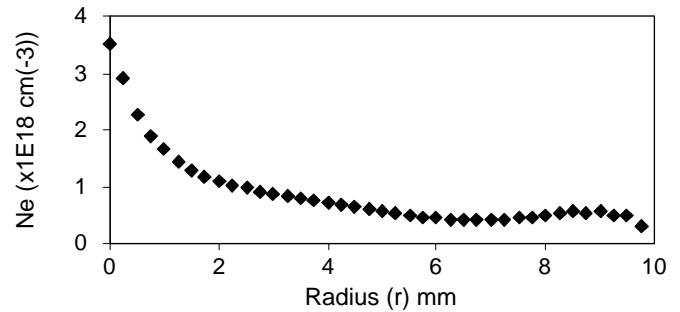
**Fig. 1.** Experimental arrangement.

the He II 1640 Å line produced by the hollow cathode lamp which is free from Stark broadening. The He-Ne laser was shone through the system at the slit of the monochromator in order to align the optical axis of the system. There are significant difficulties in making accurate wavelength measurements in the VUV region on the sources of interest [12]. A z-pinch source was used which has higher densities than those reported by most of the workers [7, 11–13]. Therefore we had a better chance to measure the shift more accurately than others did. A VUV 1-m normal incidence monochromator was employed which had a 1200 lines per mm grating with 1 m focal length blazed for 1215 Å. A solar blind Hamamatsu photomultiplier R1259 was fitted to the exit slit of the monochromator. The photomultiplier output was fed to a Tektronix AD transient digitizer and then to PDP-11/23 to record data.

It was ensured that the plasma should be viewed from the central region of the pinch with side-on configuration. The hollow cathode was continuously running during the experiment. Its signal at 1640 Å was especially checked before the scan, during the scan and after the scan. In order to ensure whether the whole system may not be misaligned with the time, we scanned the line profile for three conditions in one day and observed the clear shift of the line.

### 3 Possible errors in the measurement

In measuring the line profiles, there are inevitably some sources of errors. These errors can be attributed to both the plasma and detection system. Since the hollow cathode lamp, the z-pinch and monochromator were aligned carefully and all data for one set of conditions was taken under one set-up, the systematic errors were expected to be negligible because the shift of the Balmer- $\alpha$  line is negligible in the hollow cathode lamp. Experiments mainly

**Fig. 2.** Typical electron density distribution.

have two types of errors—errors arising from the detection system and errors due to the shot-to-shot fluctuation of the plasma source. The monochromator as a part of the detection system has its own limitations due to slight errors in the mechanical parts. In a monochromator system, the main sources of error arise from the non-uniformity of the scanning steps of the scanning motor, the mechanical and optical alignment and the illumination of the grating. In an ideal grating monochromator, small changes in the illumination of the grating affect only the width of the line [18]. In fact, the slit was used to its diffraction limit and unruled surface of the grating was also masked. This ensured that the light would diffract only from the centre of the grating rather than scatter from the unruled region. Therefore this helped to reduce any variation in the illumination across the grating.

The non-uniformity of the motor steps was checked on a number of occasions. It was found that the scanning steps lead to the error of about 0.01 Å in the position of the line. The other major error source is the shot-to-shot fluctuation of the plasma source, which is 7%. This causes an error in intensity. The variation in intensity then gives rise to an error in the half intensity point of the line. The instrument function is 0.14 Å for 20 μm slit width whereas the broadening due to Doppler effect at 40000 K is about 0.117 Å. All these errors are added up statistically to 0.02 Å for the shift measurements. The error in the case of width is about ±0.2 Å. There is an unknown error due to temperature and impurity lines.

### 4 Radial gradients effects

Normally all observed line shapes from high-density plasmas are affected by the optical depth and radial gradients. The optical depth for end-on (along the axis) for the line is greater than 1 but radially it is about 100 times less. Since the plasma was measured side-on in our case, it was optically thin. As far as the density gradient is concerned,

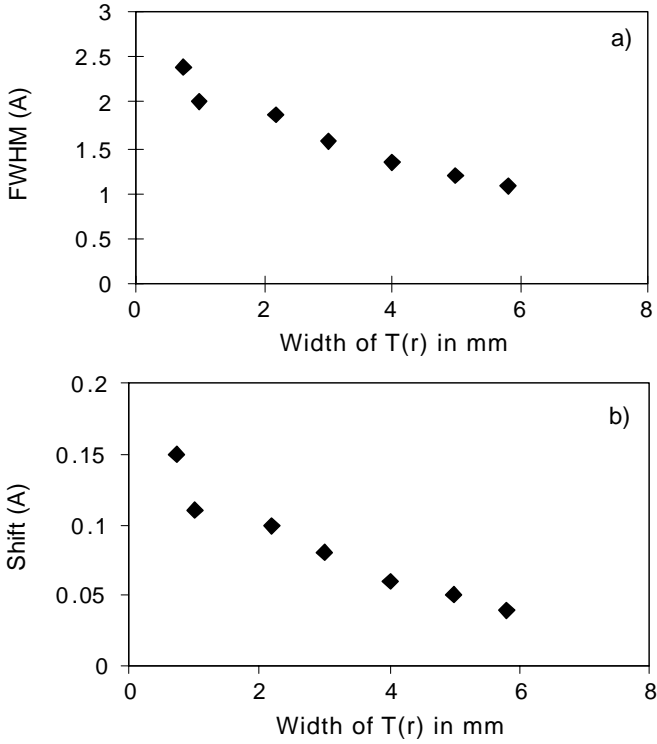


**Fig. 3.** Variation of the width and shift against different half-width of the temperature profiles (distributions).

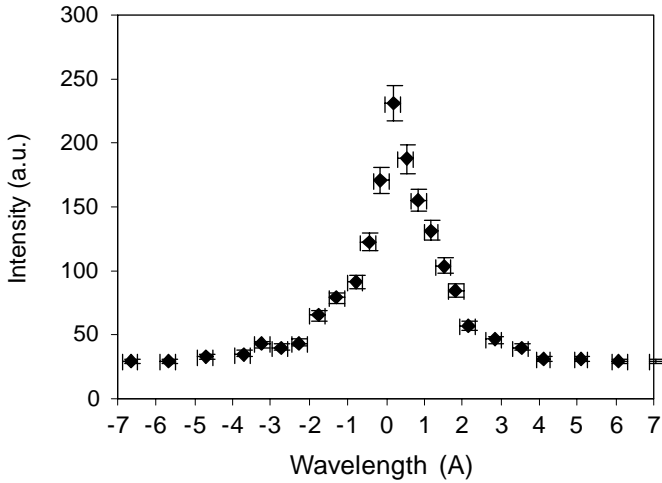


**Fig. 4.** Measured line profile at the peak diagnosed density of  $3.5 \times 10^{18} \text{ cm}^{-3}$ .

this was measured interferometrically using an argon ion laser [17] and can be seen in Figure 2. The intensity profile at He II 5876 Å using OMA was taken. The Abel inverted intensity profile was  $2.3 \pm 0.1$  mm wide at the half intensity points in contrast to the density profile (distribution) which was only 0.75 mm as shown in Figure 2. The Abel inverted temperature distribution is not reliable because of the absorption dip near line centre and the collection optics may not have defined the plasma volume well as the acceptance angle was  $f/10$ . Since the intensity (temperature) distribution is temperature-dependent, it can easily

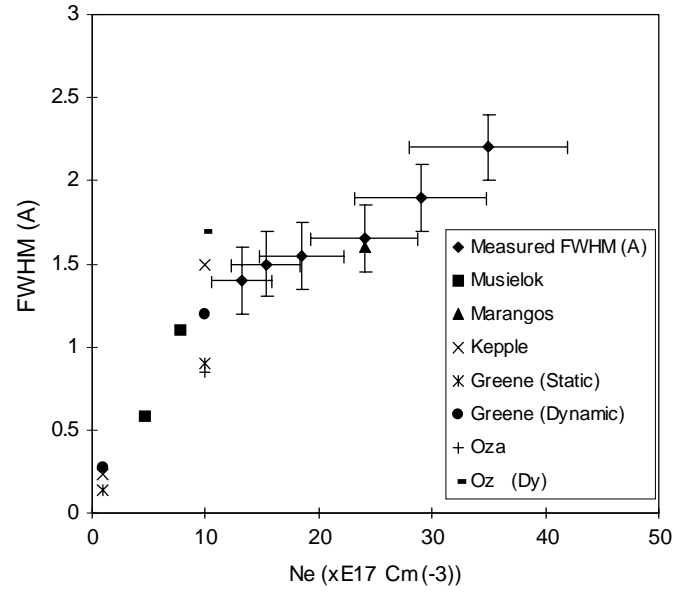


**Fig. 5.** Experimental and theoretical values of FWHM of the He II Balmer- $\alpha$  line are shown as a function of the electron density. Theoretical data:  $\times$ , ref. [4] (3.45 eV);  $\ast$ , ref. [6] (static) (8.8 eV);  $\bullet$ , ref. [6] (dynamics) (8.8 eV);  $+$ , ref. [19] (static) at 9 eV and  $-$ , ref. [19] (dynamics) at 9 eV. Experimental data:  $\blacktriangle$ , ref. [12] (3.5 eV);  $\blacksquare$ , ref. [13] (10 eV);  $\blacklozenge$ , our measurements.

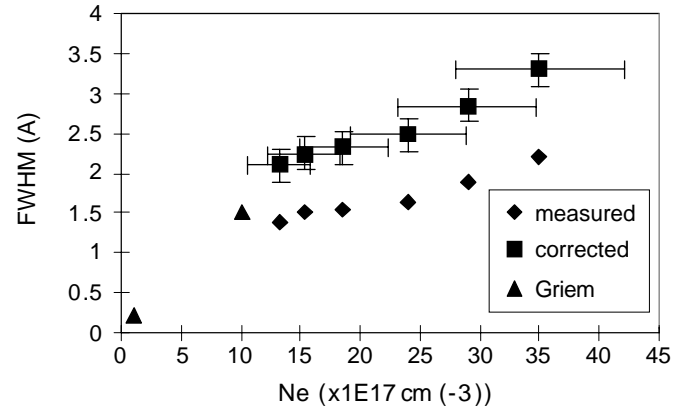


**Fig. 6.** The variation of the FWHM of the line against the electron density.  $\blacklozenge$ , measured values;  $\blacksquare$ , corrected values for radial gradients and  $\blacktriangle$ , Griem's calculated values.

be reasoned that the temperature is higher at the centre and becomes less with the radius. Therefore, it can safely be assumed that it has the same variation as that of density. The Doppler broadening depends mostly on temperature; that is why Gaussian distribution is assumed in our case. The intensity of the line with the inclusion of geometry is given by

$$\varepsilon(r, \lambda) = (hc/4\pi)A_{23}L(N_e, \lambda, T)N_3(N_e, T),$$

$$I(\lambda) = 2\pi\varepsilon(r, \lambda)r dr,$$

where  $N_e$  is known from the interferometry data and  $N_3$  is obtained by using the Saha as well as Boltzman equation. The line shape ( $L$ ) is obtained from Griem [2] (p. 302),

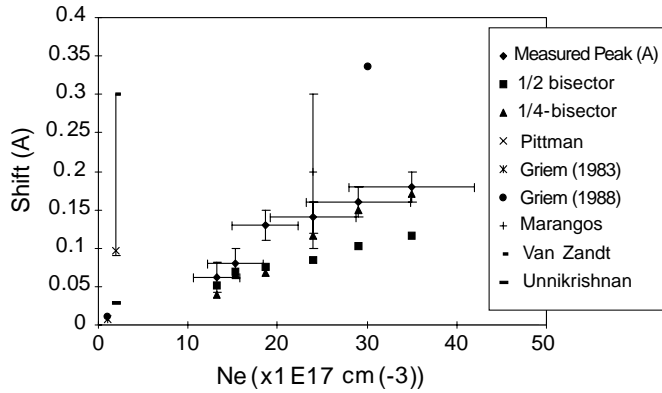


**Fig. 7.** Experimental and theoretical values of the shift of He II Balmer-alpha line are shown as a function of the electron density. Theoretical data:  $\ast$ , ref. [9];  $\bullet$ , ref. [20]; and  $-$ , ref. [8]. Experimental data:  $\times$ , ref. [7];  $+$ , ref. [12];  $\blacklozenge$ , our measured peak shift;  $\blacksquare$ , our measured shift at half-bisector and  $\blacktriangle$ , shift at 1/4-bisector.

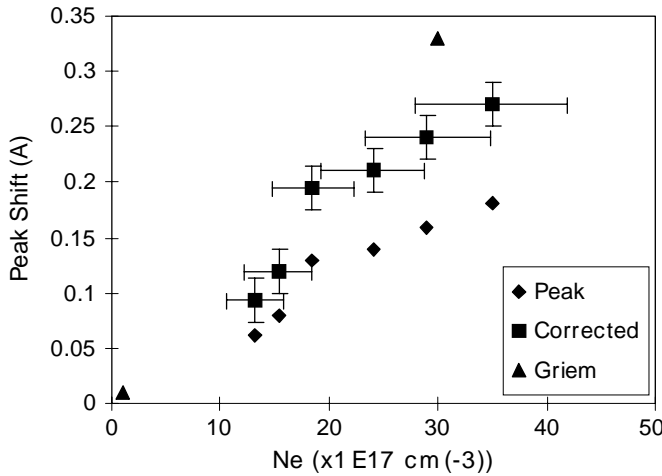


**Fig. 8.** The variation of the peak shift of the line against the electron density;  $\blacklozenge$ , measured values;  $\blacksquare$ , corrected values for radial gradients and  $\blacktriangle$ , Griem's calculated values with quadrupole shift [9].

$\varepsilon$  is the emission coefficient and  $A_{23}$  is the transition probability of the He II Balmer- $\alpha$  line. We know that the shift and width of a line vary nearly linearly with the electron density. The shift and width are introduced by fitting a straight line by using the calculated values obtained from Griem [2,9] because Griem calculated the line profile for electron densities greater than  $10^{18} \text{ cm}^{-3}$  and can be found easily in the literature.

To model the spatial gradient effects, we have developed a program which uses the calculated profile of Griem [2], our measured density distribution (Fig. 2), the model temperature distribution and impact shift from Griem [9] as inputs. The geometry of the plasma is included giving rise to the intensity  $I(r, \lambda)$  with  $g$ -weighting and then summing it over  $r$  results in  $I(\lambda)$  which is corrected for the radial density and temperature gradients.

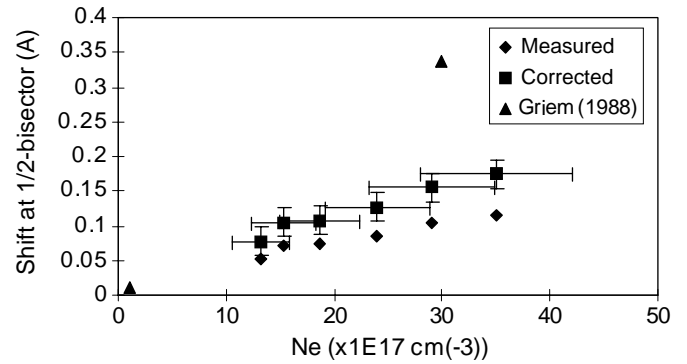


**Fig. 9.** The variation of the shift at the half-bisector of the line against the electron density;  $\blacklozenge$ , measured values;  $\blacksquare$ , corrected values for radial gradients and  $\blacktriangle$ , Griem's calculated values with quadrupole shift [9].

In Figures 3a and b, different temperature distribution have different half-widths but have the same peak temperature. The width and shift vary with the half-width of the temperature distribution. The width and shift are affected most in the region of 0 to 1 mm. This leads to the choice of temperature distribution in the program which has the half-width of 1 mm or less for the correction of radial gradient effect.

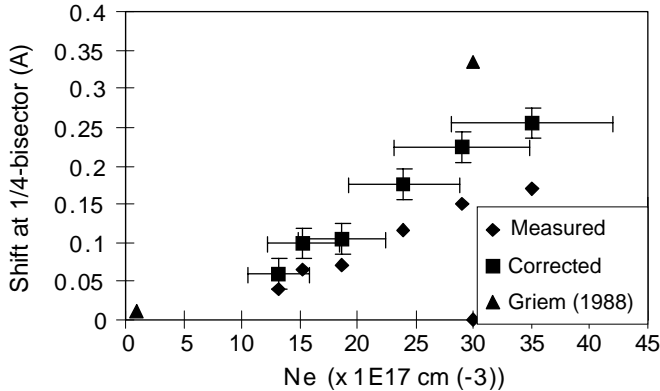
## 5 Results and discussion

The line of the He II Balmer-alpha line was measured for different plasma conditions. Each profile was found to be shifted towards the red from the centre and relative to each other with the density. The typical line profile at the density of  $(3.5 \pm 0.7) \times 10^{18} \text{ cm}^{-3}$  is shown in Figure 4. The variation of FWHM of the line against the electron density is shown in Figure 5. In this figure, we have plotted the measured and calculated width of different workers. The measured width for the profile shown in the figure is  $2.05 \pm 0.2 \text{ \AA}$ . The difference between the measured and calculated width [2] is about 80%. The difference may be due to the radial gradient effect, inherent uncertainties due to the diagnosed density and the neglect of ion dynamics. For as temperature distribution of half-width 1 mm, the corrected profile has FWHM of 3.06  $\text{\AA}$  which is about 45% smaller than Griem's profile. The measured width is then corrected to 3  $\text{\AA}$  and the difference between the measured and calculated width is about 46% (see Fig. 6). Oza [19] has investigated the effect of ion dynamics at different densities and temperature. For a density of  $(2.4 \pm 0.48) \times 10^{18} \text{ cm}^{-3}$ , the FWHM of the measured line is 1.65  $\text{\AA}$  and after correction it is found to be about 2.5  $\text{\AA}$  which is within 16% of the calculated profile of Griem [2]. The difference between calculated and measured profile is increasing with increasing density. In our case, the ion dynamics will be less than 10%. This enhanced the gap between the measured width and calculated width.

Figure 7 shows the measured and calculated shifts of different workers including ours. For the same temperature

**Table 2.** The variation of width and shift in reduced wavelength and electron density.

$N_e$ ( $\times 10^{18} \text{ cm}^{-3}$ )	1.32	1.53	1.85	2.4	2.9	3.5
FWHM ( $\times 10^{-4}$ )	9.31	9	8.2	7.6	7.8	7.6
Peak shift ( $\times 10^{-5}$ )	4.11	4	6.9	6.2	6.3	6.2

**Fig. 10.** The variation of the shift at the 1/4-bisector of the line against the electron density;  $\blacklozenge$ , measured values;  $\blacksquare$ , corrected values for radial gradients and  $\blacktriangle$ , Griem's calculated values with quadrupole shift [9].

distribution, the variation of the peak shift from the calculated shift is also around 50%. The corrected measured value is about 0.2 Å. If the linear variation of the shift is considered, then it is 20% bigger than the calculated shift [9]. Griem [20] calculated the shift for  $\Delta n = 0$  (states with the same principal quantum number ( $n$ )) which is added into  $\Delta n \neq 0$  (1983) increasing it by 33%. The shift calculated by Griem in [20] is bigger by 20% which is within the theoretical uncertainties. This is shown in Figure 7. In the case of Unnikrishnan [8], the corrected measured shift is 30 to 40% less.

Figures 8 to 10 show how the corrected measured shift of the peak, the shift at 1/2, and 1/4 intensity bisectors of the full width with reference wavelength are varying with the electron density. From these figures it can easily be found that the shift of the He II Balmer- $\alpha$  line has a nearly linear dependence on the electron density. The uncertainty in results is about 0.02 Å in the shift co-ordinate and  $\pm 20\%$  in the electron density co-ordinate.

We have tabulated the FWHM in reduced wavelength ( $\alpha$ ,  $\Delta\lambda A^{-1} \text{ cm}^{-3}$ )<sup>2/3</sup> against the electron density with  $\pm 15\%$  error and have found that if the density increases from  $1.85 \times 10^{18} \text{ cm}^{-3}$ , the FWHM remains constant. Oza and Greene [21] maintain that for hydrogen the Balmer- $\alpha$  line for Ne dependence works well in the density range from  $10^{17} \text{ cm}^{-3}$  to  $10^{18} \text{ cm}^{-3}$  and at a temperature of about 18000 K. It has been found that the shift also follows the same pattern (Tab. 2).

## 6 Conclusions

The width and shift corrected for the radial gradient effects agree well with Griem's [2,9,19] calculated value of the shift and width [2] within the uncertainty in the calculations. The measured width is 5% bigger than the calculated value of Greene (1976) while it is 20% less than the calculated value of Griem. For higher densities (Tab. 2), the width and shift of the line do not follow the linear variation. Shift values may fall into Unnikrishnan's [8] calculated values but overall it has difference of about 30% to 40% for the measured value of the shift.

I would like to thank Dr. J.P. Marangos, Prof. J.P. Conerode, and Prof. Burgess from Imperial College of Science, Technology and Medicine London for their useful criticism and help. I am also grateful to the Ministry of Science and Technology, Islamabad for providing the Scholarship.

## References

1. H.R. Griem, *Plasma Spectroscopy* (McGraw-Hill, New York, 1964).
2. H.R. Griem, *Spectral Line Broadening by Plasmas* (Academic Press, New York, 1974).
3. T. Schonig, K. Butler, *Astron. Astrophys. Suppl. Ser.* **78**, 51 (1989).
4. P.C. Kepple, *Phys. Rev. A* **6**, 1 (1972).
5. R.L. Greene, *Phys. Rev. A* **14**, 1447 (1976).
6. R.L. Greene, *J. Phys. B* **15**, 1831 (1982).
7. T.L. Pittman, C. Fleurier, *Phys. Rev. A* **33**, 1291 (1986).
8. K. Unnikrishnan, J. Callaway, D.H. Oza, *Phys. Rev. A* **42**, 6602 (1990).
9. H.R. Griem, *Phys. Rev. A* **27**, 2566 (1983).
10. B. Grabowski, J. Madej, J. Halenka, *Astrophys. J.* **313**, 750 (1987).
11. R. Van Zandt, J.C. Adcock Jr., H.R. Griem, *Phys. Rev. A* **14**, 2126 (1976).
12. J.P. Marangos, D.D. Burgess, K.G.H. Baldwin, *J. Phys. B* **21**, 3357 (1988).
13. J. Musielok, F. Bottcher, H.R. Griem, H.J. Kunze, *Phys. Rev. A* **36**, 5683 (1987).
14. R. Ahmad, *Nuovo Cimento D* **18**, 53 (1996).
15. K.G.H. Baldwin, Ph.D. Thesis, University of London, 1983.
16. D.J. Heading, Ph.D. Thesis, University of London, 1990.
17. D.J. Heading, J.P. Marangos, D.D. Burgess, *J. Phys. B* **25**, 4745 (1992).
18. R.C.M. Learner, A.P. Thorne, *J. Opt. Soc. Am. B* **5**, 2045 (1988).
19. D.H. Oza, R.L. Greene, D.E. Kelleher, *Phys. Rev. A* **37**, 531 (1988).
20. H.R. Griem, *Phys. Rev. A* **38**, 2943 (1988).
21. D.H. Oza, R.L. Greene, *J. Phys. B* **21**, L5 (1988).